Superalloys 2012: 12th International Symposium on Superalloys
Edited by: Eric S. Huron, Roger C. Reed, Mark C. Hardy, Michael J. Mills, Rick E. Montero, Pedro D. Portella, Jack Telesman
TMS (The Minerals, Metals & Materials Society), 2012

EFFECT OF THE PRIOR MICROSTRUCTURE DEGRADATION ON THE HIGH TEMPERATURE/LOW STRESS NON-ISOTHERMAL CREEP BEHAVIOR OF CMSX-4® NI-BASED SINGLE CRYSTAL SUPERALLOY

Rémi GIRAUD[1,2], Jonathan CORMIER[1], Zéline HERVIER[2], Denis BERTHEAU[1], Ken HARRIS[3], Jacqueline WAHL[3], Xavier MILHET[1], José MENDEZ[1], Antoine ORGANISTA[2].

[1] Institut Pprime, CNRS – ENSMA - Université de Poitiers, UPR CNRS 3346, Department of Physics and Mechanics of Materials, ENSMA - Téléport 2, 1 avenue Clément Ader, BP 40109, 86961 Futuroscope Chasseneuil Cedex, France
[2] Turbomeca – SAFRAN group, Materials Processes & Investigations Department, 64511 Bordes Cedex, France
[3] Cannon Muskegon Corporation, a PCC Company, Michigan, USA

Keywords: High temperature creep, Thermal cycling, γ' dissolution/precipitation, γ' rafting

Abstract

The effect of thermal cycling on the creep behavior and life of the second generation Ni-based single crystal superalloy CMSX-4® has been investigated in the very high temperature/low stress domain. Repeated overheatings at 1100°C and/or at 1150°C were introduced in the course of the creep life of the alloy at 1050°C/120 MPa. The detrimental effect of the thermal cycling compared to the isothermal creep behavior of the alloy is shown: thermal cycling leads to an increased average creep strain rate and a reduced creep life. This is always the case even when compared to the isothermal creep behavior at the highest temperature of the cycle (i.e. 1150°C/120 MPa). Moreover, the detrimental effect of the thermal cycling frequency is observed: the greater frequency the larger the creep properties decay. Compared to the first generation MC2 alloy under the same thermal cycling conditions, CMSX-4® exhibits superior non-isothermal creep properties in the very high temperature domain (T > 1100°C) due to its rhenium and γ' contents.

The effect of the microstructure degradation (i.e. γ' rafting) was also investigated by pre-straining samples at 1050°C under tension (respectively under compression) prior to creep under thermal cycling conditions. These pre-strains allowed to generate a N-type rafting (respectively P-type). N-type γ' rafting are shown to be detrimental to the non-isothermal creep properties. In contrast, P-type rafting leads to improved creep properties (i.e. reduced creep strain rate) compared to either N-type rafted or cuboidal γ' morphologies. Despite a different behavior, the creep lives are identical for both P-type rafting and the cubical γ' precipitates. From the present investigation, it is believed that: 1) P-type rafting improves non-isothermal creep properties due to a reduced dislocation climb activity 2) The transition from stationary creep to tertiary creep is controlled by the kinetics of N-type rafting.

Introduction

The constant industrial demand for increasing the performance at high temperature of aero gas turbines leads to a constant evolution to the chemical composition of nickel base superalloys [1]. The mechanical properties of Ni-based monocrystalline superalloys, especially creep, have been extensively studied over years under various isothermal conditions [2-4]. However, the operating conditions of high pressure turbine blades are far from isothermal conditions, especially in case of small uncooled HP blades of turboshaft engines for helicopters. Indeed, those components encounter different engine regimes (e.g. take off, cruise, hovering, approach …) and sometimes, unexpected emergency regimes known under the acronym OEI (One Engine Inoperative). Under such extreme conditions, the blade alloy endure short (a few seconds) very high temperature (T > 1100°C) overheating, leading to drastic microstructure evolutions as those previously analyzed by Cormier & al. [5-8]. Taking into account the effect of such OEIs or thermal cycling on the creep behavior and life of Ni-based single crystal superalloys is of prime importance for an helicopter engine manufacturer. In particular, the new certification procedures of helicopter gas turbines now include complex temperature/angular velocity histories, and sometimes thermal cycling, as for, e.g., endurance or accelerated mission (ASMET) engine tests. However, the literature analyzing the effect a such complex very high temperature creep loadings on the durability of Ni-based single crystal superalloys is scarce and mainly limited to two research teams [9-16], the pioneering works being performed on polycrystalline alloys by Rowe and Freeman [17-18]. In this context, two specific test benches were developed at the Pprime Institute (THALIE and MAATRE burners) as well as specific procedures using radiative furnaces in order to mimic realistic conditions in a controlled laboratory environment [8, 16]). This paper, will mainly be focused on the effect of thermal cycling (i.e. repeated overheatings) on the creep behavior and life of the second generation CMSX-4® alloy. A special attention will be paid to the thermal cycling frequency and to the origin of the creep rate acceleration during the "tertiary" creep stage. A comparison with the first generation MC2 alloy under similar conditions will also be performed and analyzed. Finally, the effect of the prior microstructure at the beginning of thermal cycling will be analyzed to mimic service microstructure degradation. Three kinds of microstructure will be considered: a standard cuboidal γ' microstructure (C-type structure), a γ'-rafted microstructure perpendicular to the applied tensile stress (N-type structure) and a γ'-rafted microstructure parallel to the applied tensile stress (P-type structure).

Experimental Techniques

The material mainly studied here is the second generation CMSX-4® alloy. Under some specific experimental conditions, its mechanical behavior has been compared to the first generation MC2 alloy. MC2, is an alloy often considered to be a second generation non-rhenium containing superalloy due to its superior creep properties in the 1000-1100°C temperature range (and even

better than some other second (or fourth) generation Re-containing alloys) [19, 20]. The chemical compositions of the two studied alloys are given in Table I.

Table I. Chemical compositions of MC2 and CMSX-4® alloys (Wt. %)

	Cr	Co	Al	W	Ta	Ti	Mo	Re	Hf	Ni
MC2	8	5	5	8	6	1.5	2			bal
CMSX-4®	6.4	9.7	5.64	6.4	6.5	1.05	0.6	2.9	0.1	bal

CMSX-4® samples were provided by Cannon Muskegon Company (CMC) whereas Turbomeca – SAFRAN group provided MC2 samples. CMSX-4® is heat treated following the Cannon – Muskegon solution treatment [21] and subsequent aging heat treatments of 6h at 1140°C/air quench (AQ) + 20h at 871°C/AQ. MC2 samples were solution treated for 3h at 1300°C/AQ + 4h at 1080°C/AQ and 20h at 870°C/AQ. The as-received microstructure of both alloys show approximately 70% of cubical γ' precipitates (average edge length of 0.45 µm) merged in the γ matrix. Creep specimens, 14 mm in gauge length and 4 mm in diameter were machined from single crystal rods. The strain axis is less than 5 degrees off the [001] crystallographic orientation.

Non-isothermal creep tests were performed using a radiant furnace equipped with a contactless extensometer. Reference tests on the as-received microstructure (C-type structure) were established using a reference thermal cycle described in Figure 1a and denoted in the following of the article as Type I cycling or Reference Cycle (RC) cycle. Whatever the overheating temperature, heating and cooling rates were fixed at 2°C/s and 10°C/s, respectively. The interested reader is referred to [16] for additional experimental details. All the thermal cycling considered in this article was performed using the same initial applied stress of 120 MPa. Moreover, thermal cycling (whatever its nature) was repeated until failure. The same non-isothermal creep tests were also performed using samples which were submitted to a prior isothermal creep test at 1050°C aimed at obtaining a γ' rafted microstructure. All these aged microstructures (see Table II) were composed of γ' rafts either perpendicular (N-type structure) or parallel (P-type structure) depending on the sign of the applied stress. Prior degradation under tension was performed using a constant load creep frame and a resistive furnace. Different creep durations were performed up to a well advanced secondary creep stage (i.e. 1170h at 1050°C/120 MPa) where the γ/γ' topological inversion occurred [20]. Prior creep degradation under compression was performed under constant load using an Instron 8562 machine equipped with a two zone resistive furnace and specifically developed high temperature grips to ensure perfect alignment. Creep strain was monitored using a contact extensometer. Whatever the nature of the degradation (i.e. tensile or compression), cooling at the end of the prior aging under stress was performed under load to preserve the deformation microstructure. Both a rapid thermal reloading (over 5°C/s) and a reduced soak time (5 minutes) were applied to those aged samples before launching thermal cycling, hence avoiding as much as possible any microstructure evolutions during these transient reloading stages.

Other experiments were also carried out to get a better understanding of type I non-isothermal conditions:

- the impact of the thermal cycling on the creep life was evaluated using isothermal creep tests at 1050°C, 1100°C and 1150°C under the same initial applied stress (120 MPa).
- both the effects of the overheating at the lowest temperature and the cycling frequency were investigated using type II cycling (see Figure 1b):
    - Cycle II-A : 5 min/1050°C + 1 min/ 1150°C
    - Cycle II-B : 15 min/1050°C + 1 min/1150°C
    - Cycle II-C : 30 min/1050°C + 1 min/1150°C
    - Cycle II-D : 60 min/1050°C + 1 min/1150°C

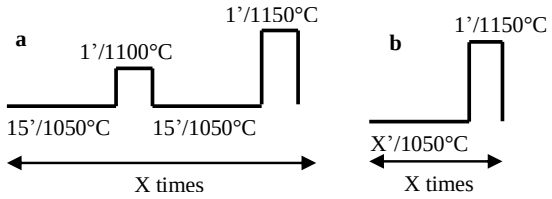

Figure 1. Type I: Reference Cycle (RC), Type II: modified cycles. These cycles were repeated X times until material failure.

Table II. Investigated prior creep degradation and prior creep strains at the end of the degradation

	Temperature (°C)	Stress (MPa)	Time (h)	Accumulated plastic strain (%)
N-type	1050	120	100	0.21
	1050	120	300	0.29
	1050	120	1170	3.4
P-type	1050	-140	140	-0.19
	1050	-141	113	-0.27
	1050	-141	113	-0.39

Microstructure investigations were performed after longitudinal sectioning, mechanical polishing up to a mirror finish. The γ/γ' microstructure was revealed by a selective dissolution of the γ' phase (the γ' phase appears in dark). Observations were performed using a Hitachi S-3500 and a JEOL 7000F Scanning Electron Microscopes (SEM), under an accelerating voltage of 25 kV.

Results

Isothermal Versus Non-Isothermal Creep Behavior

Figure 2a shows the creep curves obtained under pure isothermal conditions at 1050°C, 1100°C and 1150°C under 120 MPa and the creep curves under thermal cycling conditions using the reference cycle (see Figure 1a). Figure 2b focuses on the non-isothermal creep curves. In this figure, creep lives were normalized by the creep life obtained under thermal cycling conditions (denoted as Reference Life - RL). It can be observed from Figure 2 that thermal cycling leads to a spectacular decrease of the creep life (by a factor of 65) compared to the creep life obtained under isothermal conditions at the nominal temperature level of 1050°C. A decrease of lifetime under thermal cycling was expected since the average temperature upon thermal cycling is increased compared to 1050°C. However, it also appears that the creep life under thermal cycling conditions is reduced by a factor of ~ 2

compared to isothermal creep life at 1150°C/120 MPa (i.e. the upper temperature encountered during the temperature cycle RC). Hence, such a cyclic test cannot be considered simply as the sum of the three temperature level sequences in terms of creep life and more complex microstructure processes and history effects may control the overall non-isothermal creep behavior.

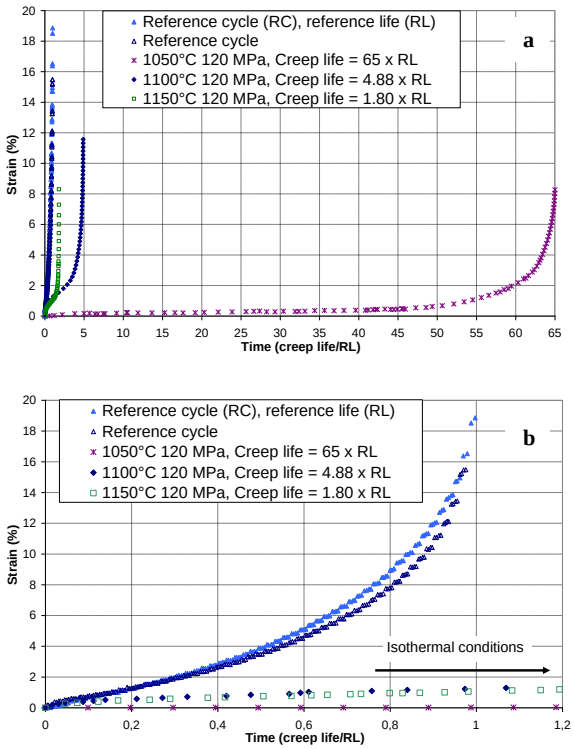

Figure 2. Creep behavior under thermal cycling conditions (type I cycling) compared to isothermal creep behaviors at 1050°C, 1100°C and 1150°C.

Compared to the isothermal creep behavior, thermal cycling promotes a very limited pseudo-steady-state creep stage and a more progressive tertiary creep stage. Actually, the tertiary stage represents a large fraction of the creep life (~ 67% of the creep life), in good agreement with the aspect of samples after creep rupture where a progressive necking along the whole gauge length is observed while a highly localized failure is obtained for the isothermal conditions.

Under such thermal cycling conditions, the average creep strain rate is increased by a factor of 1000 compared to the creep strain rate at 1050°C/120 MPa (see later analysis in Figure 9). The increase in the average creep strain rate is due to the plastic strain jumps induced by the overheatings. Figure 3 plots the evolution of these strain increments as a function of the overheating number, according to a procedure described elsewhere [16]. As expected, the higher the overheating temperature, the greater the plastic strain increment at each overheating. As observed in Figure 3, the contribution of the overheatings at 1100°C are quite insignificant (strain jumps lower than ~ 0.02%) up to the beginning of the tertiary creep stage.

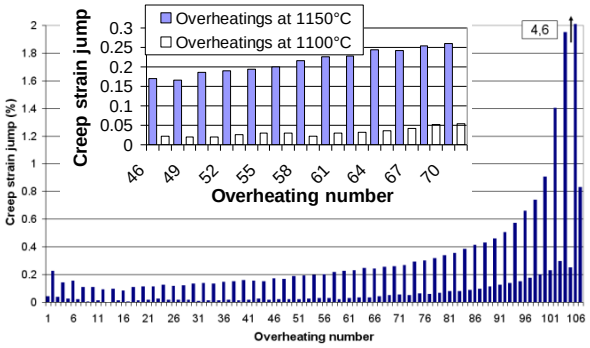

Figure 3. Evolution of the strain increment measured at each overheating during non-isothermal creep using the reference cycle with Reference Life time (RL)

It is also worth noticing that the strain increments at each overheating (both at 1100°C and 1150°C) first decrease at the beginning of non-isothermal creep test. This is believed to be due to the impact of a hyperfine γ' precipitation nucleating in the γ channels upon thermal cycling which is efficient in impeding the motion of matrix dislocations under low applied stresses [22].

Impact Of The Overheatings At 1100°C

In order to evaluate the impact of the overheatings at 1100°C during type I thermal cycling (see Figure 1a), two modified cycles were performed (Figure 4):

- an overheating at 1100°C is substituted by an overheating at 1150°C (defined as Cycle II-B).
- the 1100°C overheating (Cycle II-C) is removed.

As expected, the creep lifetime is slightly improved when the overheating at 1100°C is removed but significantly reduced if replaced by an overheating at 1150°C (Figure 4). A 25% creep life debit can be observed using Cycle II-B instead of the Reference Cycle. Interestingly, the number of cycle to failure is always reduced either when the overheating at 1100°C is removed or substituted by a 1150°C overheating (Figure 5).

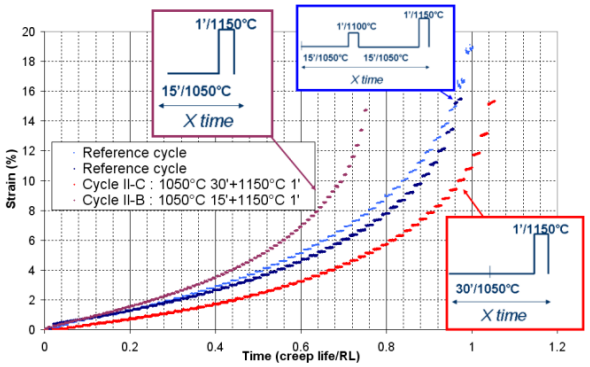

Figure 4. Effect of the thermal cycling type on the creep behavior and time to failure

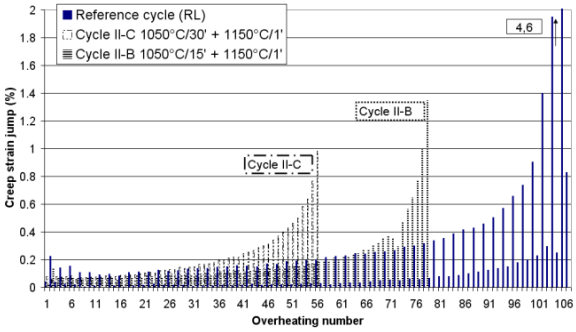

Figure 5. Evolution of the strain increment measured at each overheating during non-isothermal creep using the RL cycle, cycle II-B and cycle II-C.

Effect Of Cycling Frequency

The effect of the cycling frequency was checked out using type II thermal cycling (i.e. without any overheating at 1100°C, see Figure 1b) and varying the dwell time at the nominal 1050°C temperature. Cycles II-A, II-B, II-C and II-D were used and their respective creep behavior is presented in Figure 6.

As expected, modifying the cycling frequency promoted a drastic change in the non-isothermal creep life: the higher the frequency, the faster the average creep strain rate (if possibly defined) and the shorter the creep life (Figure 6). In addition, it becomes impossible to distinguish secondary and tertiary creep stages when increasing the cycle frequency.

Analyzing the results in terms of number of thermal cycles N_f to failure, it is observed the N_f is always higher when increasing the frequency. In other words, the material can sustain more overheatings during its entire life if the time spent at 1050°C is reduced. One interesting result is highlighted in Figure 7 when comparing N_f for cycles II-C and II-D. The main difference between these cycles is the time spent at 1050°C (30 min and 1 h respectively) leading to a reduction of the creep life by a factor 2 for cycle II-C (Figure 6). However, N_f is the same for each kind of cycle, i.e. the time spent at 1150°C is identical in both cases. As a result, in case of slow cycling, the time spent at 1150°C seems to be less detrimental than the thermal transients between 1050°C and 1150°C. These results are in good agreement with the effect of a different thermal cycling (repeated cooling in the course of a high temperature/low stress creep test). It was also shown that thermal cycling is more detrimental in terms of time to failure and strain rate compared to isothermal creep conditions and the conclusions were that the creep behavior under such conditions is highly dependent of the thermal transients [16, 23]

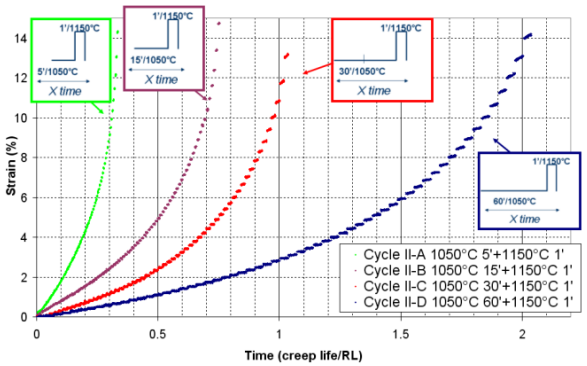

Figure 6. Effect of the cycling frequency on the non-isothermal creep properties.

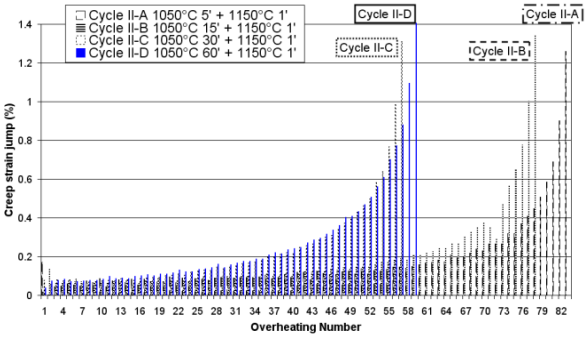

Figure 7. Evolution of the strain increment measured at each overheating during non-isothermal creep using cycles II-A, II-B, II-C and II-D.

Microstructure Evolution During Creep Under Thermal Cycling

The effect of the γ' morphology on the non-isothermal creep life has been investigated. Three microstructures were considered as defined in the experimental section: the C-structure, the N-type structure and P-type structure (Table II). These microstructures were used to investigate the possible effects of thermal cycling on the creep properties after a service microstructure degradation has been generated by regular operating conditions of a gas turbine.

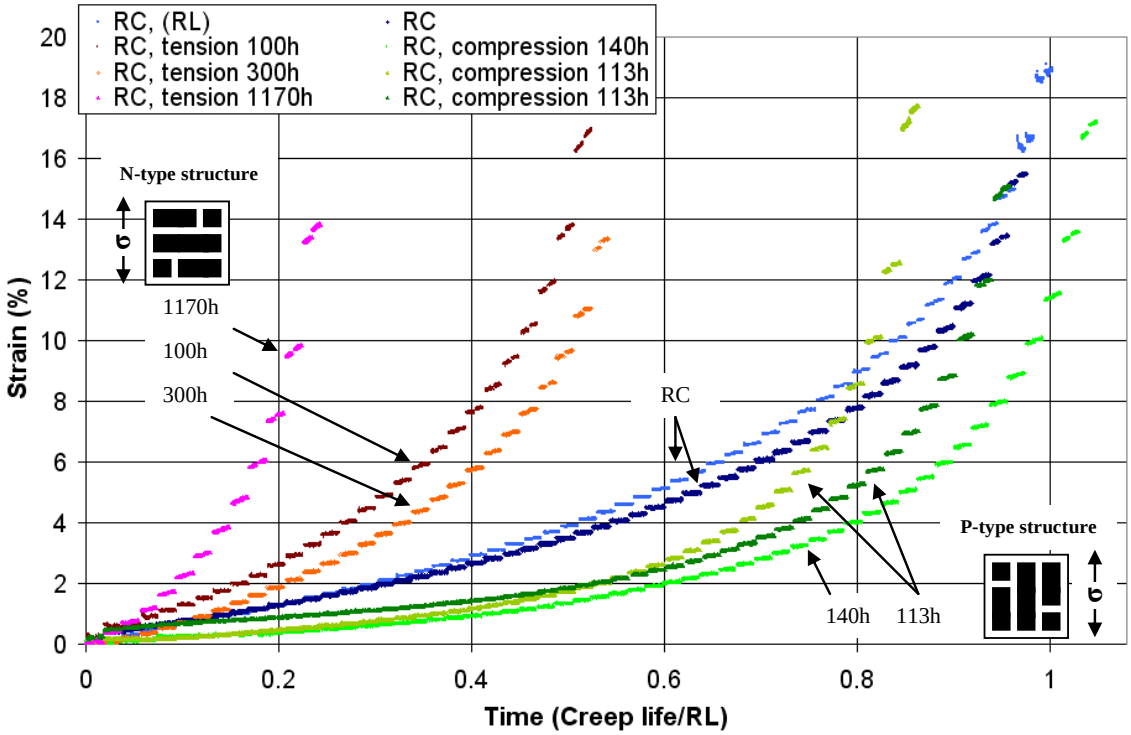

Figure 8. Effect of the γ' morphology on the creep behavior under thermal cycling conditions using type I cycle. The orientations of γ' rafts at the beginning of thermal cycling compared to the applied tensile stress appear as inserts.

Figure 8 shows the effect of the γ' morphology on the creep properties under thermal cycling using the RC cycle (see Figure 1a). The reference curve (RL) was previously presented in Figure 2b and will not require any additional comment here. As observed previously in the case of MC2 alloy [16] a detrimental effect of the N-type γ' rafting on the non-isothermal creep and life is observed for CMSX-4. It is almost impossible to define any pseudo steady-state creep stage and the creep strain is always accelerating as if the tertiary stage started at the beginning of thermal cycling. In contrast, and the most striking result of the present study, P-type γ' rafting is found to promote a long steady-state stage with a lower creep strain rate than the ones measured for both the cuboidal γ' microstructure and N-type γ'-rafted microstructure. Actually, the averaged creep strain rate with a P-type γ' rafting is found to be reduced by a factor of 2.5 as compared to a cuboidal γ' morphology and at least, by a factor of 6.5 compared to a N-type γ' rafted microstructure (Figure 9). However, for the conditions investigated in this paper, the creep life with a P-type structure at the beginning of thermal cycling is almost unchanged compared to the reference established with a virgin cubical γ' microstructure (C-type structure). This is the result of a very steep tertiary creep stage. This abrupt tertiary stage likely linked to a faster microstructure evolution occurring in these samples compared to experiments performed with both the C-type structure and N-type structure.

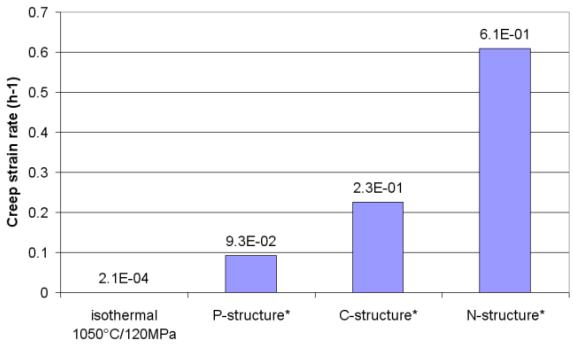

Figure 9. Creep strain rate under isothermal conditions at 1050 °C/120 MPa and for P-type structure, for C-structure and for N-type structure under type I thermal cycling. *Averaged value over all the database

Microstructure Characterizations

As-received and degraded γ/γ' microstructures (C-type structure, N-type structure and P-type structure respectively) are presented in Figures 10a, 10b and 10c, respectively. For sake of simplicity, only one γ/γ' degraded microstructure per kind of γ' rafting (i.e. N- or P-type) will be presented since the fundamental mechanisms of γ' evolution during creep under thermal cycling are qualitatively identical. The chosen prior creep degradation for

microstructure inspections are: 300h at 1050°C/120 MPa for the N-type structure and 140h at 1050°C/-140 MPa for the P-type structures. For a better understanding, the tensile stress applied during the thermal cycling part of the creep tests has been superimposed in Figure 10.

Microstructures observed after creep failure in the necking sections and away from the necking sections are presented in Figures 10(d-f) and Figures 10(g-i) respectively.

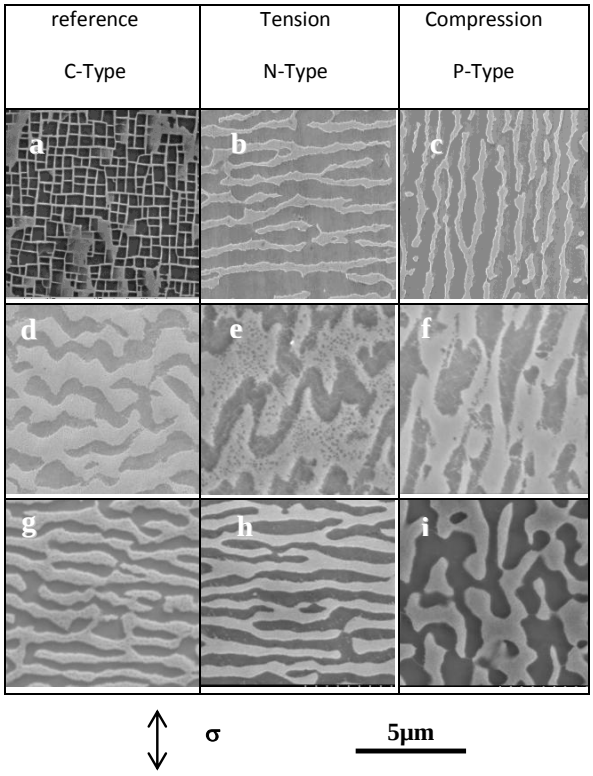

Figure 10. γ/γ' microstructures observed using the SEI mode after surface polishing and subsequent chemical etching for each kind of microstructure degradation observed at the beginning of thermal cycling (a-c), after creep failure in the necking section (d-f) and after creep failure out of the necking section (g-i)

In the necking sections, the γ' rafts are highly wavy for the C and N-type structure (Figures 10d and 10e, respectively). In contrast, the originally vertical γ' rafts of the P-type structure seems to remain parallel to the applied tensile stress, even if slightly coarsened (Figures 10f). Away from the necking sections, C and N-type structures exhibit a classical γ'-rafted structure perpendicular to the tensile stress axis (Figures 10g and 10h) whereas the P-type structure exhibits a highly disturbed microstructure (Figure 10i), resulting from a progressive fragmentation and re-orientation of the originally vertical rafts, as already observed elsewhere under isothermal conditions [24-26]. Comparing Figures 10f and 10i, it is believed that the morphology of γ' particles elongated parallel to the tensile stress axis in the necking section of an initially P-type rafted microstructure results from the three dimensional stress state obtained in the late stages of creep deformation close to failure.

Comparison Of The Non-Isothermal Creep Behavior With MC2 Alloy

The typical creep behaviors of the first generation MC2 alloy [16] and CMSX-4®are compared in Figure 11, under type I thermal cycling. A C-type structure at the beginning of thermal cycling is investigated here. As expected, type I thermal cycling is more harmful to the MC2 creep properties compared to the rhenium containing CMSX-4® alloy creep. Both a faster creep strain deformation during pseudo-secondary creep stage and steeper tertiary creep stages are observed for MC2 alloy. Moreover, MC2 alloy exhibits a reduced strain to failure compared to CMSX-4® alloy.

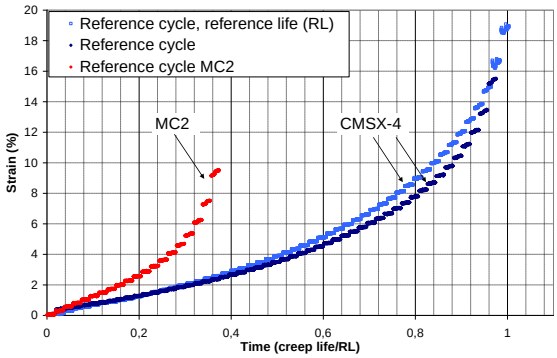

Figure 11. Non-isothermal creep behaviors of the first (MC2) and second (CMSX-4®) generation superalloys using type I thermal cycling, i.e. non-isothermal conditions.

Discussion

Impact Of The Material's Chemistry On The Non-Isothermal Creep Properties

Numerous studies have demonstrated the beneficial effect of the addition of 3% (wt %) rhenium in second generation Ni-based superalloys on the isothermal creep properties in a wide temperature range compared to first generation alloys [19, 21, 27]. This effect is once again checked here under non-isothermal conditions (Figure 11). However, it requires to be analyzed in depth. Indeed, MC2 exhibits better isothermal creep properties than CMSX-4® (lower secondary creep strain rate and increased creep life) in the high temperature/low stress creep domain (e.g. 1050°C/120 MPa, the reference level here studied). This is mainly due to its very fast N-type γ' rafting under such isothermal conditions. In fact, the γ' rafts of MC2 are very stable and not prone to coarsening or topological inversion [20]. Hence, the decreased non-isothermal creep strength of MC2 alloy compared to CMSX-4® clearly highlights once again that the operative damage mechanisms under such non-isothermal creep conditions are different from those operating under isothermal conditions. Therefore, a robust design, taking into account such harsh non-isothermal conditions requires a different approach than those based solely on isothermal conditions [7].

One of the major difference between MC2 and CMSX-4® lies in the Re content. Re is known, among other things, to slow down the diffusion processes [28, 29] such as the γ' directional

coarsening [30]. In fact, the rafting process ends after 24h at 1050°C/120 MPa for MC2 (Re- free) and after 100h for CMSX-4® under similar conditions [16, 31]. Since a cuboidal γ/γ' microstructure is more resistant to non-isothermal creep than a N-type rafted one (this point will be analyzed later in the discussion), it is believed that part of the CMSX-4® advantage over MC2 is due to this slower N-type γ' directional coarsening. Therefore, the better resistance to γ' rafting is believed to be one of the key parameter resulting in the better non-isothermal creep performance of CMSX-4. However, once γ' rafting completes, one may also question the impact of thermal cycling (i.e. of γ' dissolution/precipitation) on their stability (i.e. the propensity of the γ/γ' interfaces for becoming more or less wavy, see e.g. Figure 10e). This point is under investigation.

The other important creep-controlling parameter under such very high temperature conditions is the γ' volume content at thermodynamic equilibrium [32, 33]. The plots of the γ' volume fraction at thermodynamical equilibrium for both MC2 and CMSX-4® alloys in the interesting temperature domain of this study clearly highlight a greater fraction for CMSX-4® in all the temperature range and a higher γ' solvus (Figure 12).

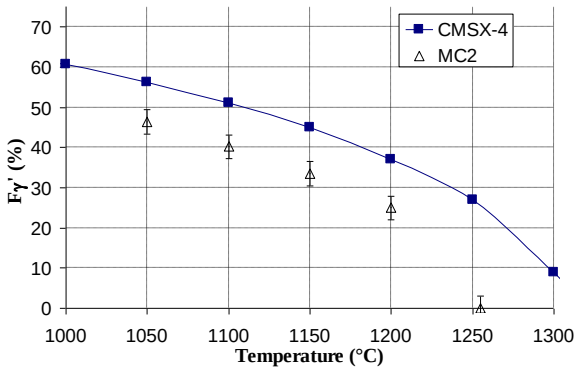

Figure 12. γ' volume fraction of MC2 and CMSX-4® alloys. CMSX-4 data extracted from [34]

Therefore, under thermal cycling conditions, since the dissolution kinetics of CMSX-4® are slower than that of MC2 ones [6, 31] and since the γ' volume content at equilibrium is higher for CMSX-4®, a higher γ' content remains at the end of an overheating for CMSX-4® compared to MC2. This entails larger areas of γ/γ' interface and thinner γ channels for CMSX-4® during the overheatings. Dislocation climb and Orowan bowing processes are therefore likely to be more efficiently slowed down in case of CMSX-4®. This leads to smaller creep strain increments at each temperature jump for CMSX-4® and then to both a slower creep strain rate and an increased creep life.

Effect Of Cycling Frequency

It is observed from Figure 4 that the introduction of 1100°C overheating does not change drastically the non-isothermal creep behavior of CMSX-4® alloy. Its creep behavior under such non-isothermal conditions is mainly controlled by two parameters: 1) the way the thermal cycling is performed (i.e. heating and cooling rates, cycling frequency) and 2) the upper temperature during overheatings (i.e. 1150°C in the present case). The overheating at 1100°C was shown to contribute only to the creep deformation when the tertiary creep stage begins.

When analyzing only the type II cycling, it appeared that the faster the cycling is, the smaller is the creep life (Figure 6). This result is quite logical since increasing the cycling frequency basically corresponds to an increase in the average temperature of the test. However, the detrimental effect of thermal cycling cannot be linked only to an increase of the average temperature since other kind of thermal cycling (i.e. cooling in the course of a high temperature creep test) also leads to a decrease in the creep properties [9-13, 23]. It is believed that the thermal transitions (i.e. heating and cooling) have a strong contribution to the increased creep strain rate in, e.g., forcing dislocations to enter the γ'-phase [35], and, by analogy, as also observed by L. Dirand following a stress jump during high temperature creep test in the 950-1150°C temperature range [36]. It is also interesting to notice from Figure 7 that the slower thermal cycling tests (type II-C and II-D cycles) have almost the same creep life in terms of number of cycles up to failure (N_f) while the creep duration is twice (30 min of dwell time at 1050°C compared to 1 h). Hence, the time spent at 1150°C seems to be less detrimental than the thermal transients between 1050°C and 1150°C. As a result, the time during which the microstructure is out of equilibrium, both in terms of γ' volume fraction and local dislocation densities [5, 15], appears to be the most critical parameter in controlling N_f. Comparing type II-C and II-D thermal cycling, it is possible to assume that 30 minutes at 1050°C is long enough to reach a new microstructure equilibrium after a 1150°C overheating, both in terms of γ' content [31] and dislocation densities (either at the γ/γ' interfaces or in the γ' phase). A longer time at 1050°C does not change N_f since the creep strain rate in the later parts of the dwell times at 1050°C is nearly zero. In the case of faster cycling (cycles II-A and II-B), the microstructure is always away from equilibrium and both dislocation climb and Orowan bowing processes are easier due to a lower average γ' content. Moreover, in increasing the cycling frequency, γ' rafting is probably faster, so that all of these three processes that lead to faster creep deformation are active and produce a reduced creep life.

Effect Of The Prior Microstructure Degradation

The γ/γ' microstructure degradation in the form of a N-type γ' rafting was previously demonstrated to be detrimental to a number of mechanical properties such as tensile properties [37] or high temperature low-cycle fatigue ones [38-40]. Under LCF loads, N-type γ' rafting was shown to provide faster crack propagation rates compared to a cuboidal γ/γ' microstructure or to a P-type γ' rafted one (i.e. microstructure with a more tortuous crack path), hence leading to lower LCF lives [38, 39]. The only case under which such a directional coarsening is often considered is creep under high temperature/low stress, i.e. under conditions where γ' cutting by dislocations is not the prominent deformation mechanism [34, 41]. In fact, even if impossible to demonstrate unambiguously, N-type γ'-rafting has often been considered to be beneficial to the (isothermal) high temperature/low stress creep properties in impeding efficiently dislocation climb.

Under the presently investigated conditions, representative of some engine operating conditions, it is demonstrated that N-type rafting is detrimental. This is also true for MC2 alloy [16]. In fact,

the observations of the γ' microstructure at failure of the C-type structure clearly demonstrate that a N-type rafting occurred (Figures 10e and 10h). Figure 8 also suggests that the progressive transition from a pseudo "secondary" creep stage to the tertiary creep stage is mainly controlled by the N-type γ' rafting kinetics or, in the case of an initially P-type rafted microstructure, to the kinetics of fragmentation and re-orientation of the γ' particles perpendicular to the tensile stress axis.

The other interesting result of the present article is the initial lower creep strain rate of the P-type structure compared to both the C-type structure and the N-type structure (see Figures 8 and 9). According to Tetzlaff and Mughrabi, [24], and under the present low stress conditions, the P-type structure should be the most creep resistant due to its larger areas of vertical γ/γ' interfaces where the dislocation climb process is impeded most strongly. This lower creep strain rate compared to a cuboidal γ/γ' microstructure and to a N-type γ' rafted one is maintained as long as fragmentation of the vertical plates is avoided. However, once this fragmentation has occurred and that subsequent γ' particle reorientation occurs, the creep properties dwindle, leading to a very steep tertiary creep stage (see Figure 8). Fortunately in the present case, the creep life is similar to the one observed for the C-type structure. Since the γ' fragmentation/re-orientation of a P-type γ' microstructure is more time dependant than stress dependent [24], it is expected that an increase in applied stress will increase the non-isothermal creep life. This point is under investigation.

Conclusions

The effect of thermal cycling on the high temperature/low stress tensile creep properties of CMSX-4® has been investigated as a function of the γ' precipitation degradation. Different kinds of thermal cycling were investigated, including overheatings at 1100°C and/or 1150°C and different frequencies in the course of creep at 1050°C/120 MPa. Moreover, three kinds of microstructures prior to thermal cycling were investigated: a standard as-received cuboidal γ' precipitation, a N-type γ'-rafted microstructure (i.e. normal to the applied tensile stress) and a P-type γ'-rafted microstructure (i.e. parallel to the applied tensile stress).
The main conclusions that can be drawn from the present investigation are:

1. Thermal cycling is detrimental to both the creep strain rate and creep life of the alloy, even compared to the isothermal creep properties of the alloy at the highest temperature encountered during thermal cycling (i.e. 1150°C/120 MPa).
2. A higher thermal cycling frequency leads to an increased average creep strain rate and to a reduced creep life.
3. CMSX-4® alloy is more resistant to non-isothermal creep than MC2 alloy, probably due to both a greater γ' content in the upper temperature domain (T > 1100°C) and to its rhenium content.
4. N-type γ' rafting is deleterious to the non-isothermal creep properties.
5. Under the investigated conditions, P-type γ' rafting has been found to improve the non-isothermal creep properties by decreasing the creep strain rate by a factor of 2.5 as compared to a cuboidal morphology and by a factor of at least 6.5 compared to a N-type γ' rafted microstructure. Under the investigated conditions (especially in applied stress), non-isothermal creep life has been found to be insensitive the prior degradation under compression.
6. Compared to the initial γ/γ' microstructure and to γ' rafts perpendicular to the applied stress, the improved non-isothermal creep strain rate with γ' rafts parallel to the applied stress are due a dislocation climb process more strongly impeded due to larger areas of vertical γ/γ' interfaces.
7. The creep life under such non-isothermal conditions seems to be highly depend on the kinetics of γ' rafting perpendicular to the applied tensile stress, even with a prior P-type rafting where γ' rafts tend to split and reorient perpendicular to the applied stress.

Acknowledgements

The authors are grateful to Turbomeca – SAFRAN group for sponsoring this work and for RG PhD thesis grant. Florence Hamon is gratefully for her kind assistance in several experiments.

References

1. G.L. Erickson, "The Development and Application of CMSX-10", *Superalloys 1996*, ed. R. Kissinger, D.J. Deye, D.L. Anton, A.D. Cetel, M.V. Nathal, T.M. Pollock and D.A. Woodford, (Warrendale, PA: The Minerals, Metals & Materials Society, 1996), 35-44.

2. A. Epishin, et al., "New technique for characterization of Microstructural degradation under creep: Application to the nickel-base superalloy CMSX-4", *Materials Science Engineering A*, 510-511 (2009), 262-265.

3. A. Ma, D. Dye, and R.C. Reed, "A model for the creep deformation behaviour of single-crystal superalloy CMSX-4", *Acta Materialia*, 56 (2008), 1657–1670.

4. D.W. MacLachlan, and D.M. Knowles, "Modelling and prediction of the stress rupture behaviour of single crystal superalloys", *Materials Science Engineering A*, 302 (2001), 275-285.

5. J. Cormier, X. Milhet, and J. Mendez, "Non-isothermal creep at very high temperature of the nickel-based single crystal superalloy MC2", *Acta Materialia*, 55 (2007) 6250–6259.

6. J. Cormier, X. Milhet, and J. Mendez, "Effect of very high temperature short exposures on the dissolution of the γ' phase in single crystal MC2 superalloy", *Journal of Materials Science*, 42 (2007) 7780–7786.

7. J. Cormier, and G. Cailletaud, "Constitutive modeling of the creep behavior of single crystal superalloys under non-isothermal conditions inducing phase transformations", *Materials Science and Engineering A*, 527 (2010) 6300–6312.

8. J. Cormier et al., "Simulation of Very High Temperature Overheating During Isothermal Creep of Single Crystal Ni-Base Superalloy", *Advanced Engineering Materials*, 10 (1-2) (2008), 56-61.

9. A. Raffaitin et al., "The effect of thermal cycling on the high-temperature creep behaviour of a single crystal nickel-based superalloy", *Scripta Materialia*, 57 (2007), 277-280.

10. F. Touratier et al., "Rafting microstructure during creep of the MC2 nickel-based superalloy at very high temperature", *Materials Science and Engineering A*, 510–511 (2009) 244–249.

11. M. Hantcherli et al., "Evolution of interfacial dislocation network during anisothermal high-temperature creep of a nickel-based superalloy", *Scripta Materialia*, 66 (2012) 143–146.

12. R. Goti, B. Viguier, and F. Crabos, "Thermal cycling creep behaviour of single crystal nickel-based superalloy", (Paper presented at the 12th international conference on creep and fracture of engineering materials structures, Kyoto, Japan, May 2012).

13. R. Goti, B. Viguier, and F. Crabos, "Effect of thermal cycling on high temperature creep of coated CMSX-4", *Superalloys 2012*, ed. R.C. Reed, M. Hardy, E.S. Huron, M. Mills, R. Montero, P. Portella and J. Telesman, (Warrendale, PA: The Minerals, Metals & Materials Society, 2012).

14. J. Cormier, X. Milhet, and J. Mendez, "Anisothermal creep behavior at very high temperature of a Ni-based superalloy single crystal", *Materials Science and Engineering A*, 483–484 (2008) 594–597.

15. J. Cormier et al., "Non-isothermal creep behavior of a second generation Ni-Based single crystal superalloy: experimental characterization and modeling", *Superalloys 2008*, ed. R.C. Reed, K.A. Green, P. Caron, T.P. Gabb, M.G. Fahrmann, E.S. Huron and S.A. Woodard, (Warrendale, PA: The Minerals, Metals & Materials Society, 2008), 941-949.

16. J. Cormier et al., "Very high temperature creep behavior of a single crystal Ni-based superalloy under complex thermal cycling conditions", *Philosophical Magazine Letters*, 90 (8) (2010), 611–620.

17. J.P. Rowe, and J.W. Freeman, "Effect of overheating on creep-rupture properties of HS-31 alloy", (Final report project 1478-10, Engineering Research Institute, University of Michigan, 1956).

18. J.P. Rowe, and J.W. Freeman, "Effect of overheating on creep-rupture properties of M252 and Inconel 700 alloys at 1500°F and 1600°F", (Final report project 02846, Engineering Research Institute, University of Michigan, 1960).

19. P. Caron, "High γ' solvus new generation nickel-based superalloys for single crystal turbine blade applications", *Superalloys 2000*, ed. T.M. Pollock, R.D. Kissinger, R.R. Bowman, K.A. Green, M. McLean, S. Olson, and J.J. Schirra (Warrendale, PA: The Minerals, Metals & Materials Society, 2000), 737-746.

20. P. Caron, C. Ramusat, and F. Diologent, "Influence of the γ' fraction on the γ/γ' topological inversion during high temperature creep of single crystal superalloys", *Superalloys 2008*, ed. R.C. Reed, K.A. Green, P. Caron, T.P. Gabb, M.G. Fahrmann, E.S. Huron and S.A. Woodard, (Warrendale, PA: The Minerals, Metals & Materials Society, 2008), 159-167.

21. K. Harris et al., "Development of the Rhenium containing for single crystal blade and directionally superalloys CMSX-4® & CM 186 LC® solidified vane applications in advanced turbine engines", *Superalloys 1992*, ed. S.D. Antolovich, R.W. Stusrud, R.A. MacKay, D.L. Anton, T. Khan, R.D. Kissinger, D.L. Klarstrom, (Warrendale, PA: The Minerals, Metals & Materials Society, 1992), 297-306.

22. J.-B Le Graverend et al., "Effect of fine γ' precipitation on non-isothermal creep and creep-fatigue behaviour of nickel base superalloy MC2", *Materials Science and Engineering A*, 527 (2010) 5295–5302.

23. B. Viguier et al., "Microstructure evolution and deformation mechanisms during thermal cyclic creep of a single crystal nickel based superalloy", (Paper presented at the 16th International Conference on Strength of Materials, Bangalore, India, august, 2012).

24. U. Tetzlaff, and H. Mughrabi, "Enhancement monocristalline of the high-temperature tensile creep strength of nickel-base superalloys by pre-rafting in compression", *Superalloys 2000*, ed. T.M. Pollock. R.D. Kissinger, R.R. Bowman, K.A. Green, M. McLean, S. Olson, and J.J. Schirra, (Warrendale, PA: The Minerals, Metals & Materials Society, 2000), 273-282.

25. T. Sugui et al., "Deformation features of a nickel-base superalloy single crystal during compression creep", *Materials Science and Engineering A*, 379 (2004) 141–147.

26. Y. Xingfu et al., "Microstructure evolution of a pre-compression nickel-base single crystal superalloy during tensile creep", *Materials Science and Engineering A*, 506 (2009) 80–86.

27. A.D. Cetel, and D.N. Duhl, "Second-generation nickel-base single crystal superalloy", *Superalloys 1988*, ed. S. Reichman, D.N. Duhl, G. Maurer, S. Antolovich and C. Lund, (Warrendale, PA: The Minerals, Metals & Materials Society, 1988), 235-244.

28. M.S.A. Karunaratne, P. Carter, and R.C. Reed, "Interdiffusion in the face-centered cubic phase of the Ni–Re, Ni–Ta and Ni–W systems between 900 and 1300°C", *Materials Science and Engineering A*, 281 (2000) 229 – 233.

29. C.E. Campbell, W.J. Boettinger, and U.R. Kattner, "Development of a diffusion mobility database for Ni-base superalloys", *Acta Materialia*, 50 (2002) 775–792.

30. W.Z. Wang et al., "Role of Re and Co on microstructures and in single crystal superalloys γ' coarsening," *Materials Science and Engineering A*, 479 (2008) 148–156.

31. R. Giraud et al., "Strain effect on the γ' dissolution at high temperatures of a Nickel-based single crystal superalloy", *Metallurgical and Materials Transactions A*, Submitted for publication.

32. T. Murakumo et al., "Creep behaviour of Ni-base single-crystal superalloys with various γ' volume fraction", *Acta Materialia*, 52 (2004) 3737–3744.

33. R.C. Reed, The Superalloys - Fundamentals and Applications (Cambridge, UK: Cambridge University Press, 2006).

34. R.C. Reed, D.C. Cox, and C.M.F. Rae, "Damage accumulation during creep deformation of a single crystal superalloy at 1150 ◦C", *Materials Science and Engineering A*, 448 (2007) 88–96.

35. J.-B Le Graverend et al., "*In situ* measurement of the γ/γ' lattice mismatch evolution of a nickel-based single crystal superalloy during non-isothermal very high temperature creep experiments", *Metallurgical and Materials Transactions A*, Submitted for publication.

36. L. Dirand, "Fluage à haut température d'un superalliage monocristallin: expérimentation *in situ* en rayonnement synchrotron", (Ph.D. Thesis, INP Lorraine, Ecole des Mines de Nancy, 2011).

37. M. Nazmy et al., "Environmental effects on tensile and low cycle fatigue behavior of single crystal nickel base superalloys", *Scripta Materialia*, 48 (2003) 519–524.

38. M. Ott, and H. Mughrabi, "Dependence of the high-temperature low-cycle fatigue behaviour of the monocrystalline nickel-base superalloys CMSX-4 and CMSX-6 on the γ/γ' morphology", *Materials Science and Engineering A*, 272 (1999) 24–30.

39. H. Mughrabi, M. Ott, and U. Tetzlaff, "New microstructural concepts to optimize the high-temperature strength of γ'-hardened monocrystalline nickel-based superalloys", *Materials Science and Engineering A*, 234-236 (1997) 434-437.

40. A. Epishin et al., "Creep damage of single-crystal nickel base superalloys: mechanisms and effect on low cycle fatigue", *Materials at high temperatures*, 27 (1) (2010), 53-59.

41. H. Mughrabi, and U. Tetzlaff, "Microstructure and high-temperature strength of monocrystalline Nickel-base superalloys", *Advanced Engineering Materials*, 6 (2) (2000), 319-326.